MSc in Photonics

PHOTONICS**BCN**

Universitat Politècnica de Catalunya (UPC)
Universitat Autònoma de Barcelona (UAB)
Universitat de Barcelona (UB)
Institut de Ciències Fotòniques (ICFO)

http://www.photonicsbcn.eu

Master in Photonics

MASTER THESIS WORK

Entangled Photon Source for Single Molecule Microscopy

Soroush Abbasi Zargaleh

Supervised by Prof. Niek Van Hulst, (ICFO)

Presented on date 11th February 2013

Registered at

Escola Tècnica Superior d'Enginyeria de Telecomunicació de Barcelona

Entangled Photon Source for Single Molecule Microscopy

Soroush Abbasi Zargaleh

Molecular Nanophotonic Group, ICFO – The Institute of Photonic Sciences, Mediterranean Technology Park Av. Carl Friedrich Gauss, 3 08860 Castelldefels (Barcelona), Spain

E-mail: soroush.abbasizargaleh@icfo.es

Abstract. This paper presents experimental implementation of highly correlated photons for single molecules microscopy application. We designed and built a Type-II Spontaneous Parametric Down Conversion (SPDC) photon pair source for coupling with a home-built dual objectives microscope. Further, we measured biphotons polarization dependence signals with a pair of state projector.
Keywords: Entangled Photon, SPDC, Microscopy.

1. Introduction

Interest in detection and probing single molecules for investigation and manipulation has been the driving force for invention of new techniques in this field. In this context, techniques such as NSOM [1], STORM [2], PALM [3] and recently plasmonic nanoscale devices has been developed over the past years. As single molecules size are smaller than diffraction limit, the demand for more precise and efficient detection techniques beyond the diffraction limits is inevitable, which require more sophisticated single molecule approaches.

Almost all single molecules techniques avail substantial number of uncorrelated photon. The ply of large uncorrelated photon is common in all above techniques which deviates from reaching goal of obtaining maximum possible information from smallest number of employed photons in order to move toward more precise and efficient techniques. However, investigation of higher order correlation in near-field has been a theoretical hypotheses due to challenges in generation of highly correlated photon with sufficiently large photons yield. Further, exploiting such highly correlated photons for probing single molecules without destroying their correlation due to perturbation during manipulation of single molecules and detection of such photons with sensitivity at single photon level still remains a great challenge. Furthermore, coupling of such photons to nanoscale devices to detect single molecules and detection of it is a challenge to overcome. Entangled photon pairs are generally important for the realization of quantum communication, computation [4], cryptography [5] and teleportation [6, 7, 8]. Our basic objective is to investigate and develop photon pairs that can be interfaced with a dual objective microscope for next-generation single molecule techniques and applications. In this context, generation of high fidelity entangled photons, coupling of such delicate photons to plasmonic nano-structures for enhance probing of single molecules and preservation of their quantum states after coupling to such nano-scaled structures is a milestone.

The paper is organized as follows: Section 2 gives an brief overview on quantum entanglement, EPR paradox, Bell's inequality theoretical description, and CHSH inequality for experimental purposes. Section 3 describes the quantum mechanical description of pure, mixed and entangled states, Section 4 presents experimental setups, Section 5 presents the experimental results and analysis which follows by conclusion.

2. Quantum Entanglement

Quantum entanglement is a quantum mechanical phenomenon in which the quantum states of two or more particles become related in a way such that any change of state made to one of the particle affects the state of the other particle. Entanglement coined by Schrödinger [9] is a form of quantum superposition which according to the Copenhagen interpretation of quantum mechanics,

their shared state is indefinite until measured, which collapses their shared state into separable states.

2.1. Einstein, Podolsky, Rosen (EPR)

This peculiarity in quantum mechanics was highlighted by Einstein, Podolsky, and Rosen in their seminal paper [10] (known as EPR Paradox), they believed entanglement is due to ineptness of quantum mechanics. They developed a thought experiment intended to reveal what they believed to be inadequacies of quantum mechanics by illustrating that quantum theory could not describe certain intuitive "elements of reality" and thus was not a complete physical theory. This so-called "EPR Paradox" has led to much subsequent, and still ongoing research.

According to EPR view, in a complete theory "there is an element corresponding to each element of reality" and element of physical reality is an element whose value can be precisely predicted without disturbing the system. EPR believed in Local Realism and their two main assumptions were ; Realism - the world exists independently of our observations and Locality - objects cannot affect one another instantaneously through a distance. Their thought experiment was based on the concept that two events cannot influence each other if the distance between them is greater than the distance light could travel in the time available. However, The quantum formalism allows one to envisage a peculiar situations where measurements performed on one of spatially separated pair of entangled particles is indirect measurement of second particle in the sense that from the outcome of the first measurement one can deduce with probability 1 a property of second particle, since the two systems are strongly correlated. It seems that entangled particles can apparently have an instantaneous influence on one another and affect the outcome of measurement. This effect is now known as "nonlocality". They argued that quantum mechanics cannot explain this effect without violating the locality principle. EPR raised the question that if it is possible to explain the probabilistic character of quantum predictions by invoking supplementary unknown parameters ? They postulated the existence of such supplementary unknown parameters and coined them as "hidden variables", thus they should account for the discrepancy. Their claim was that quantum meachanics theory is incomplete since it does not completely describe physical reality. Furthermore, they claimed that these hidden variables would be local, so that no instantaneous action at a distance would be necessary. Niels Bohr strongly opposed to EPR conclusion on existence of Local Hidden Variables (LHV) theory. His interpretation is known as the "Copenhagen Interpretation" of quantum mechanics.

2.2. Bell's Inequality

EPR seemed to encompass a more complete description that would obliterate the indeterminacy of quantum mechanics by introducing local hidden-variable theories. In hidden variable theory, measurement is actually fundamentally deterministic, but perceive to be probabilistic due to our lack of knowledge of the hidden variables.

In 1964, John Bell [11] proposed a theorem to verify the existence of hidden variables based on EPR concept which showed that either the statistical predictions of quantum theory or the principle of locality is incorrect. Since quantum mechanical predictions cannot be reproduced by local hidden variable theories, Bell did not conclude which one was false but only that both cannot be true at the same time.

We consider the proposed experimental setup as described for the EPR-paradox by Bohm [12] in which two particles which originate from a comon source and propagate in opposite directions towards their corresponding measurement apparatuses and detectors. Let λ be set of hidden variables and $p(\lambda)$ its probability distribution determining the measurement results for any possible measurement setting. In contrast, the quantum mechanical probabilistic measurement results are explained by the paucity of statistical distribution $p(\lambda)$. According to Bell's original approach [11], the result A of the spin measurement on particle 1 was taken to depend on $\hat{a}$, $\hat{b}$, and λ as $A(\hat{a}, \hat{b}, \lambda)$. Similarly, $B(\hat{a}, \hat{b}, \lambda)$ represents the result of a spin measurement on the particle 2. Bell, then, applied Einstein's locality (i.e. the act of measurement on particle 2 with via measurement setting $\hat{b}$ is a local event which does not affect the measurement result A of particle 1) in the

following form:

$$A(\hat{a},\hat{b},\lambda) = A(\hat{a},\lambda),\ B(\hat{a},\hat{b},\lambda) = B(\hat{b},\lambda) \tag{2.1}$$

Two different measurement outcomes are provided for one particle by $A(a,\lambda), A(a',\lambda)$ and for the other one by $B(b,\lambda), B(b',\lambda)$, where a, a' and b, b' are adjustable parameters which characterize the measurement apparatuses ($\hat{a}$, e.g., is the direction of magnetic field in a Stern-Gerlach experiment). The measurement results are deterministic functions since they depend on λ. The possible measurement results are:

$$A(\hat{a},\lambda) = \pm 1,\ B(\hat{b},\lambda) = \pm 1 \tag{2.2}$$

The principle of locality requires $A(a,\lambda), A(a',\lambda)$ being independent of $B(b,\lambda), B(b',\lambda)$ and vice versa. This is ensured by a spatial separation of the measurement apparatuses. Consequently, The expectation value for a joint measurement on both particles given by a local realistic theory can therefore be written as

$$E(\hat{a},\hat{b}) = \int_{\Lambda} p(\lambda)A(\hat{a},\lambda)B(\hat{b},\lambda)\ \mathrm{d}\lambda \ \textit{with} \int_{\Lambda} p(\lambda)\ \mathrm{d}\lambda = 1,\ p(\lambda) \geq 1 \tag{2.3}$$

Since the $p(\lambda)$ is normalized probability distribution

$$A(\hat{a},\lambda) = -B(\hat{b},\lambda) \tag{2.4}$$

Equation (2.3) can be rewritten in following form

$$E(\hat{a},\hat{b}) = -\int_{\Lambda} p(\lambda)A(\hat{a},\lambda)A(\hat{b},\lambda)\ \mathrm{d}\lambda \tag{2.5}$$

For another measurement setting for particle 2 in unit vector $\hat{c}$ direction using Equations (2.2) one obtains :

$$|E(\hat{a},\hat{b}) - E(\hat{a},\hat{c})| \leq \int_{\Lambda} p(\lambda)|A(\hat{a},\lambda)A(\hat{b},\lambda)[A(\hat{b},\lambda)A(\hat{c},\lambda) - 1]|\ \mathrm{d}\lambda \tag{2.6}$$

equivalently written as

$$|E(\hat{a},\hat{b}) - E(\hat{a},\hat{c})| \leq 1 + E(\hat{b},\hat{c}) \tag{2.7}$$

which is the reputed Bell inequality. The only assumption is that the hidden variable theory is subject to perfect measurement apparatus and perfect anti-correlation (based on EPR concept on spin measurement for a spin 1/2 singlet state), Equations (2.2) and (2.4), respectively. This mathematical restriction on local realistic theories is the original form of Bell's inequality. It is satisfied by all local hidden variable models regardless of the measurement directions. The above local realistic model should reproduce the quantum mechanical expectation value given by

$$E_{QM}(\hat{a},\hat{b}) = \left\langle \psi^{-} \middle| \sigma_1.\hat{a} * \sigma_2.\hat{b} \middle| \psi^{-} \right\rangle = -\hat{a}.\hat{b} \tag{2.8}$$

However, quantum mechanics maximally violates Equation (2.7), if the unit vectors are chosen such that $\hat{a}$ and $\hat{b}$ are orthogonal and $\hat{c}$ makes an angle of 45° degrees with both $\hat{a}$ and $\hat{b}$. In this case, we have $\hat{a}.\hat{c} = 0$ and $\hat{a}.\hat{b} = \hat{b}.\hat{c} = -1/\sqrt{2}$. Inserting their quantum mechanical expectation value obtained from Equation (2.8) in Bell's inequality one obtains

$$1/\sqrt{2} \leq 1 - 1/\sqrt{2} \tag{2.9}$$

These results are irrefutable violation of Bell's inequality which implies that there does not exist any local hidden variable theory consistent with these outcomes of quantum mechanics. Thereafter, experiments by Freedman and Clauser [13], Aspect, Dalibard, and Roger [14] and others confirmed that quantum theory prediction explains the experimental measurements and the principle of local events could not explain the experimental results.

2.3. Clauser, Horn, Shimony and Holt (CHSH) Inequality

In this section we will derive a slightly more general version of Bell's inequality known as the Clauser-Horne inequalities. These were first proposed in 1969 by Clauser, Horn, Shimony and Holt (CHSH)[15] to arrive at an inequality that would be more suitable for experimental testing. The derivation of Bell's theorem was based on the perfect correlation.

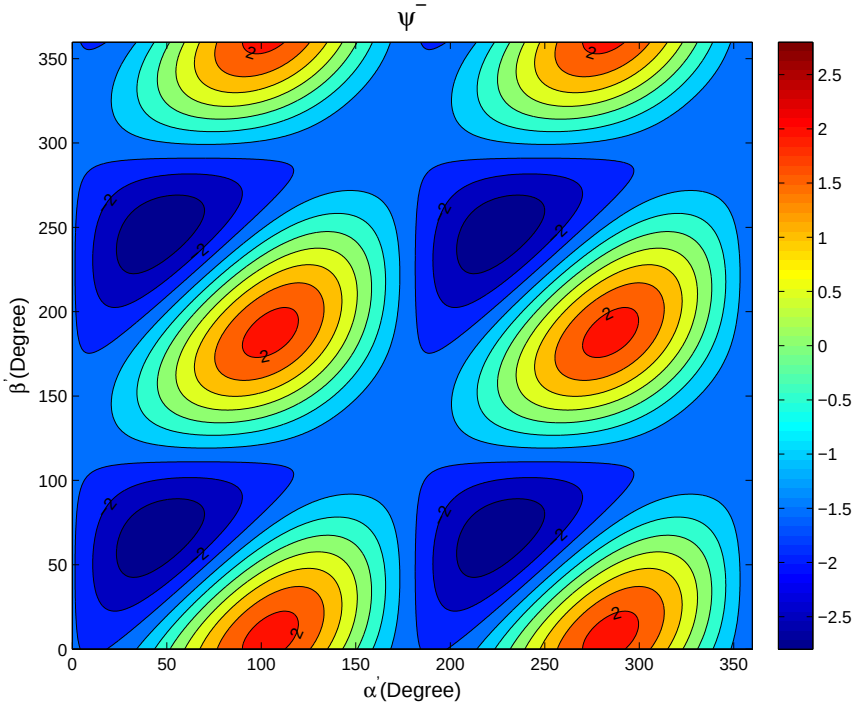

Figure 1: Numerical calculation of CHSH inequality for set of four angles for full measurement of S. For calculation, $\alpha = 0°$ and $\beta = 22.5°$ set to a fix value and S calculated as a function of both α' and β', when $|S| = 2\sqrt{2}$ result in a maximum violation of CHSH inequality.

In an experiment, these would require perfect measurement devices and a perfectly pure $|\psi^-\rangle$ state, which are not possible in experimental context. In 1974, Clauser and Horn [16] further derived an inequality based on Bell's theorem, which does not require perfect correlations and is thus applicable for experiments [15]. In practical aspect, CHSH inequality allows measurement devices to fail to register one or both particles contrary to Bell's original inequality that the measurement devices are assumed to be perfect.

Instead of the perfect measurement results assumption (2.2) in Bell's inequality we use the average value of the outcomes $\bar{A}(\hat{a}, \lambda)$ and $\bar{B}(\hat{b}, \lambda)$ and since the possible values of A and B are 1, 0 and +1, it follows that:

$$|\bar{A}(\hat{a}, \lambda)| \leq 1, \ |\bar{B}(\hat{b}, \lambda)| \leq 1 \tag{2.10}$$

for two alternative measurement directions $\hat{a}'$ and $\hat{b}'$, we have

$$E(\hat{a}, \hat{b}) - E(\hat{a}, \hat{b}') = \int_\Lambda p(\lambda)[\bar{A}(\hat{a}, \lambda)\bar{B}(\hat{b}, \lambda) - \bar{A}(\hat{a}, \lambda)\bar{B}(\hat{b}', \lambda)] \, \mathrm{d}\lambda \tag{2.11}$$

and using (2.10) one can obtains

$$|E(\hat{a}, \hat{b}) - E(\hat{a}, \hat{b}')| \leq 2 \pm E(\hat{a}', \hat{b}') - E(\hat{a}', \hat{b}) \tag{2.12}$$

by rearranging the terms in a more symmetric form, one obtains the CHSH inequality as following

$$S(\hat{a}, \hat{b}, \hat{a}', \hat{b}') = |E(\hat{a}, \hat{b}) - E(\hat{a}, \hat{b}')| + |E(\hat{a}', \hat{b}) + E(\hat{a}', \hat{b}')| \leq 2 \tag{2.13}$$

For fixed angles α and β, where, depending on both α' and β', CHSH's inequality can be expected to be violated. Figure 1 illustrates numerical calculation of full measurement of S parameter based on set of 4 angles for Bell state ψ^-.

3. Quantum States

3.1. Pure and Mix States

In quantum theory, pure quantum states are described by finite-dimensional complex vectors on the Hilbert space $\mathcal{H}$

$$|\Psi\rangle = \sum_x a_x |x\rangle \in \mathcal{H} = C^n \tag{3.1}$$

However, from experimental aspect this is not the most general state since states are usually not pure as they cannot be completely isolated from the surrounding environment. Therefore, one has to consider mixed states which are statistical ensemble of pure states. A general mixed state can be described by density matrices through an incoherent superposition of pure states

$$\rho = \sum_n p_n |\Psi_n\rangle \langle\Psi_n| \tag{3.2}$$

where the p_n are a probability distribution for the states $|\Psi_n\rangle$ accordingly. Normalized density matrices [17] satisfy

$$\rho^\dagger = \rho \ , \ Tr(\rho) = 1 \ , \ \rho \geq 0 \tag{3.3}$$

where the last inequality is an operator inequality which indicates that all eigenvalues of ρ are nonnegative.

3.2. Entangled States

A pure quantum state is called separable if only it can be written as a direct product

$$|\Psi_{sep}\rangle = \left|\Psi^A\right\rangle \otimes \left|\Psi^B\right\rangle \tag{3.4}$$

where $\left|\Psi^A\right\rangle \in \mathcal{H}_A$ and $\left|\Psi^B\right\rangle \in \mathcal{H}_B$ are the states of the systems A and B respectively, Otherwise, they reside in a same Hilbert space, this state called entangled and has the following form

$$|\Psi_{ent}\rangle = \sum_i c_i \left|\Psi_i^A\right\rangle \otimes \left|\Psi_i^B\right\rangle \tag{3.5}$$

with at least two non-vanishing complex coefficients c_i. In the case of mixed state, a density matrix ρ is separable if only there exists at least one decomposition of the form

$$\rho = \sum_n p_n \ \rho_n^A \otimes \rho_n^B \tag{3.6}$$

while for an entangled state there is no decomposition into separable states.
There are four possible states with maximum entanglement for a pair of photons with two possible orthogonal H (horizontal) and V (vertical) polarizations basis. These four states are named Bell states and defined as a maximally entangled quantum state of two qubits ;

$$\left|\psi^-\right\rangle = \frac{1}{\sqrt{2}}(|HV\rangle - |VH\rangle) \tag{3.7}$$

$$\left|\psi^+\right\rangle = \frac{1}{\sqrt{2}}(|HV\rangle + |VH\rangle) \tag{3.8}$$

$$\left|\phi^-\right\rangle = \frac{1}{\sqrt{2}}(|HH\rangle - |VV\rangle) \tag{3.9}$$

$$\left|\phi^+\right\rangle = \frac{1}{\sqrt{2}}(|HH\rangle + |VV\rangle) \tag{3.10}$$

There are various schemes for generation of entangled photons such as single trapped atoms, atomic ensembles and Four Wave Mixing (FWM). In this investigation we utilized Spontaneous Parametric Down Conversion (SPDC) in χ^2 non-linear crystals which is one the most convenient way for generating entangled photons. Generally, the SPDC process divides into several categories based on the polarization of the pump and generated downconverted photon;
Type-0 : Pump and both down-converted photons are co-polarized.
Type-I : Down-converted photons are co-polarized but orthogonal to pump polarization.
Type-II : The signal and idler photons have orthogonal polarization. In this process, the input pump photon down converted into two photons, momentum and energy are conserved, with appropriate scheme to make the photon pair indistinguishable one can achieve polarization entangle state for generated pair photons.

4. Experimental Setup

In our experimental setup, we employed Type-II SPDC in a periodically poled potassium titanyl phosphate KTiOPO4 (ppKTP) nonlinear crystal which benefits from Quasi-phase matching (QPM) scheme that eases the momentum conservation condition, placed in center of a polarization Sagnac interferometer (PSI). The built experimental setup consist of CW and Ultrafast stages capable of inline operation. The ultrafast setup composed of Ti:Sapphire ultrafast laser working in femtosecond regime, its output is doubled by BiBO crystal, after precise alignment of Ti:Sapphire cavity, the pulse dispersion compensated by inline autocorrelation technique and coupled into the Sagnac interferometer with help of dichroic pulse combiner. The CW experimental setup consist of an up-conversion stage based on bowtie ring cavity which is made of two planar mirrors and two curved mirrors with a nonlinear crystal place at focal point of the curve mirrors for generation of pump photon at 397nm. The up-converted pump coupled into a polarization Sagnac interferometer as a down-conversion stage for generation of highly correlated photons which one of its output further coupled into a home built dual-objective microscope stage and reach to detection stage, the second output directly coupled to a detection stage. The detection stage consist of polarization analyzer modules for analyzing the states of generated photons and Single Photon Avalanche Detectors (SPAD) with low level dark counts of approximately 7 counts per second. The PSI source has been under investigation [18, 19, 20].

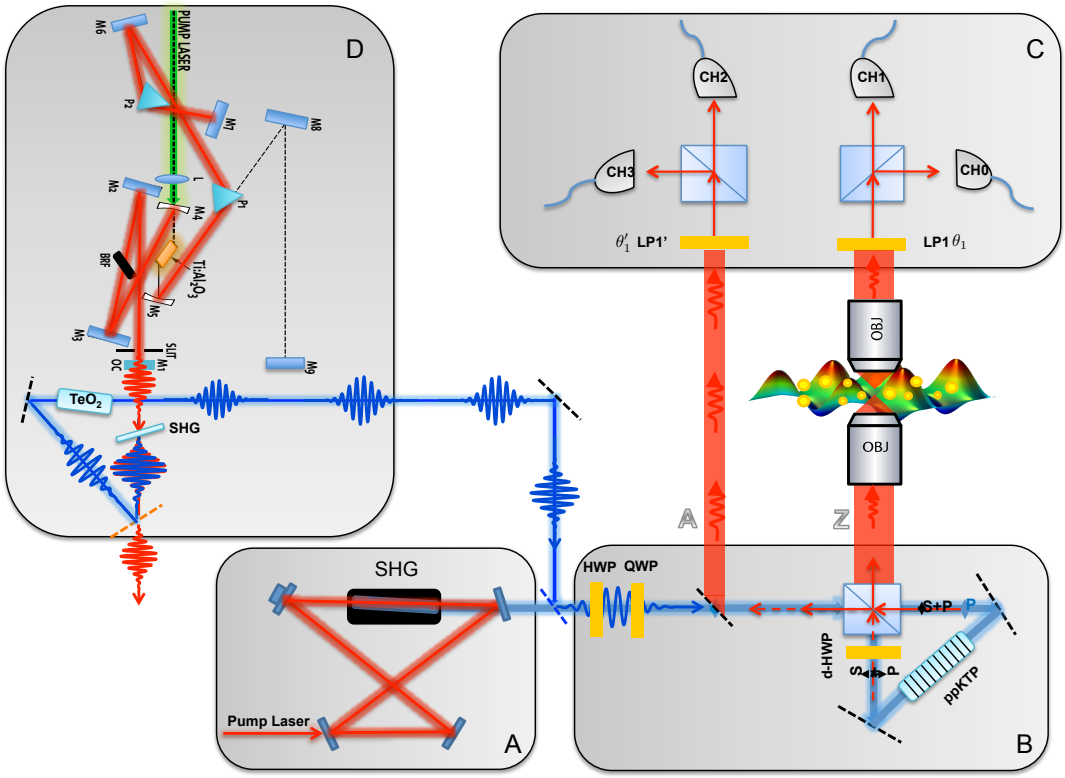

Figure 2: Experimental Setup : A. The active mode-locked bow-tie ring cavity with a SHG BiBO crystal as nonlinear medium for generation 397nm laser. B. Polarization Sagnac interferometer for the generation of polarization entangled photon pairs. C. The quantum state analyzer D. Ultrafast source of polarization entangled photon pairs.

In this section, a brief introduction to working principle of the CW part of experimental setup as shown in Figure 2 is presented. The injected input pump laser with 397 nm wavelength is split into orthogonal polarization components at the dual-wave polarizing beam splitter (dPBS) at the interferometer input. The counter clockwise propagating part of the pump laser generates a signal and idler photon with 794 nm wavelength and with horizontal (H) and vertical (V) polarization, respectively (Figure 2.B). Their polarization is rotated by 90° after passing a dual-wavelenght half

wave plate (dHWP) such that the idler photon (now H-polarized) is transmitted at the dPBS and leaves the interferometer through output Z (perpendicular to optical table surface). The V-polarized signal photon gets reflected at the dPBS and, using a dichroic mirror, it is separated from the pump laser and reflected to output A. The polarization of the clockwise propagating component of the pump laser is rotated by 90° at the d-HWP and also generates a H-polarized signal photon and a V-polarized idler photon at 794 nm (Figure 2.B). The clockwise propagating V-polarized idler photon gets reflected at the dPBS and leaves the interferometer through output Z. Similarly, the clockwise propagating H-polarized signal photon is transmitted at the dPBS and leaves the interferometer through output A. If the polarization of the pump laser is chosen, such that half of the intensity gets reflected and half transmitted at the dPBS. The output is entangled state in the two output modes A and Z:

$$|\psi_\phi\rangle = \frac{1}{\sqrt{2}}(|H_i\rangle\,|V_s\rangle + e^{i\phi}\,|V_i\rangle\,|H_s\rangle) \tag{4.1}$$

The phase ϕ originates from the phase relation between the vertical and horizontal components of the pump laser field and the individual phases added up by the down-conversion fields in the interferometer.

This phase can be manipulated via a half wave plate (HWP) and a quarter wave plate (QWP) in the pump laser beam (Figure 2.B). A half wave plate (HWP) before the ppKTP in a rotary mount allows the control of pump polarization. The phase angle ϕ can be adjusted by tilting a quartz quarter wave plate (QWP) placed before the ppKTP. This tunes the entanglement state of the down-converted photons. The QWP is mounted on a rotation stage for precise tilting. In our experiment, the phase was adjusted such that we obtained the maximally entangled Bell state

$$\left|\psi^-\right\rangle = \frac{1}{\sqrt{2}}(|H_i\rangle\,|V_s\rangle - |V_i\rangle\,|H_s\rangle) \tag{4.2}$$

The photons at the outputs were collimated and coupled to microscope stage, which were connected to the quantum channels consisting of 4 Single Photon Avalanche Detectors (SPAD) during the measurements, transmitting the photons to A and Z, respectively. Each beam has an adjustable polarizer in front of the SPADs in order to measure photons with the configured polarization. Both beams are focused onto the detectors using a pair of lens to shrink the beam diameter and effectively increase its intensity onto the small active area of the SPADs. The signals of the detectors are sent to a coincidence counter and sent to a workstation for further processing.

5. Measurement and Analysis

The photon states were generated in the CW setup shown in Figure 2.B the cw pump laser beam ($\lambda = 397nm$) incident on 10 mm long ppKTP-crystal and pairs of entangled photons are produced. The generated photons have orthogonal polarization and wavelengths of around $\lambda = 794nm$ due to parametric down conversion type-II phase matching condition. In order to detect only the entangled photon pairs generated from spontaneous parametric down-conversion (SPDC), we used a pair of narrow-band filter with FWHM of 12 nm centered at 800nm, which also prevent the avalanche photodiodes from being deluge by photons that were not in the wavelength region of interest. The entangled photon pairs are post selected by the conditional detection with single-photon detectors. In the course of experiment, we measured SPDC photon pairs signal based on their polarization with single photon detector. We used a pair of polarizer mounted on rotational mount to transform the polarization states of SPDC photons. The polarizer act as wavefunction projector on photon pairs which can be described in terms of vectors corresponding to its transmission and extinction directions. One can represent the horizontally and vertically polarized states of photons as $|H\rangle$ and $|V\rangle$, respectively, the polarizer with its transmission axis forming an angle θ with the horizontal axis will transform the photon states into the new basis states

$$|T_\theta\rangle = cos\theta\,|H\rangle + sin\theta\,|V\rangle \tag{5.1}$$

and the state of transmitted photon will become

$$|T_\theta\rangle\,\langle T_\theta\,|\,\psi\rangle \tag{5.2}$$

As we have mentioned, the type-II down conversion of our experiments generates two polarized photons, that is, in the state $|\psi\rangle$. In an experiment, the generated photon pair beams went directly

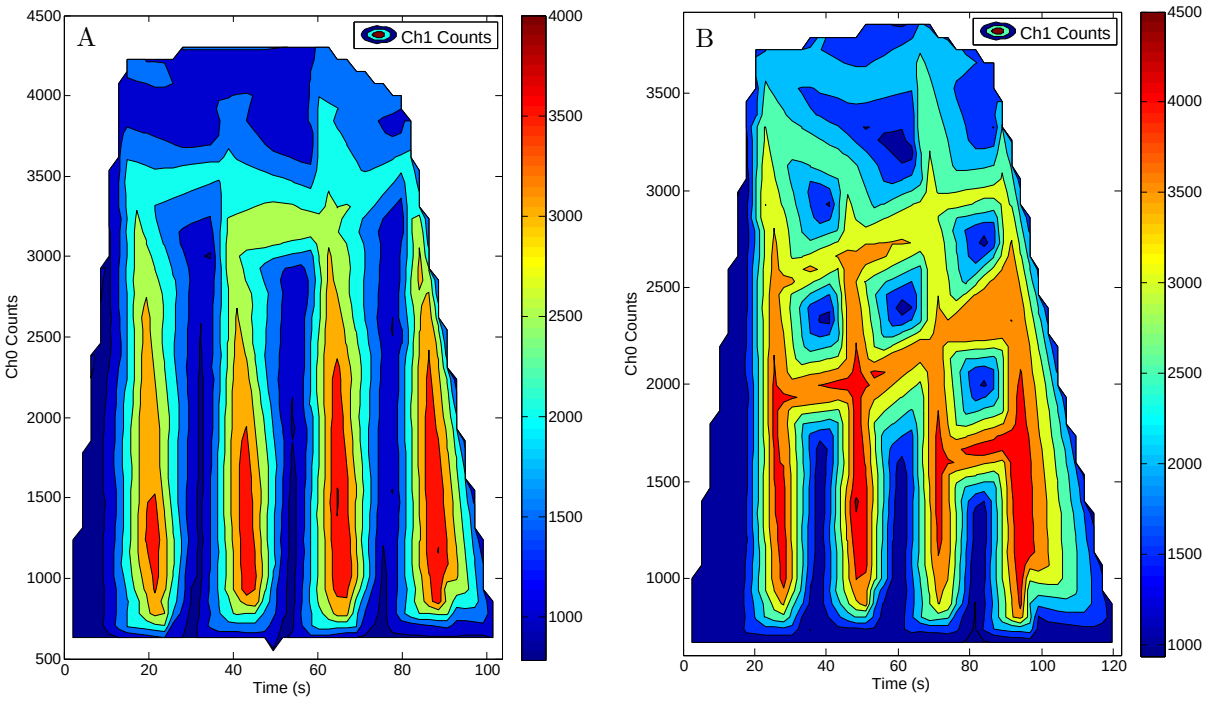

Figure 3: Entangled photon pair counts : A. Polarizer LP1' transmission axis set to horizontal by setting $\theta_1' = 0$ and varied the angle θ_1 of the second polarizer from 0 to 4π. B. Polarizer LP1' transmission axis set to diagonal by setting $\theta_1' = 0$ and varied the angle θ_1 of the second polarizer from 0 to 4π.

to the detectors, we placed a rotational polarizer, labeled LP1' and LP1, on the path of the photon pair as shown in Figure 2.C. We set polarizer LP1' with its transmission axis horizontal that is, $\theta_1' = 0$, and varied the angle θ_1 of the second polarizer from 0° to 360° and recorded the SPDC counts on the channel 0 and 1 as a function of the LP1 angle θ_1. In a second measurement, with the same setting as pervious experiment we only modified the polarizer LP1' transmission axis from horizontal to diagonal by setting $\theta_1' = 45°$ and recorded the SPDC counts on the channel 0 and 1 as a function of the LP1 angle by varying θ_1 in similar manner as previous measurement. The UV pump power adapted in the experiment was about $Pp \approx 65uW$. At such a low power typically 4500 counts per second were detected.

In the case of non-correlated photons, the photons pair are assumed to be independent. Therefore, the measurement result in both measurement scenario should yield the same result since the polarizer setting of one channel should not affect the result of other channel. As illustrated in Figure 3, there is shown evidence for biphoton polarization dependence with a large contrast between Ch0 and Ch1 counts distributions as in Figure 3.A. Whereas, in Figure 3.B the degree of visibility between two detection channels is reduced significantly due to change in counts distributions on each channels. By comparing experimental measurement results, we observe that the results are not similar in both measurements as one would expect in the case of non-correlated photons. Nonetheless, there is no change in polarizer configuration of Ch0 and Ch1 respect to first measurement the count distribution has been reshaped. We further calculated numerical expected detection probability of the photon pair for different configurations of the polarization setting based on locality assumption and plotted the simulation results in Figure 4. The simulation result can only explain the experimental result obtained in the first measurement based on assumption of the independent uncorrelated photons. If the generated photon pair state is separable then the photon pair detection probability should explain the results in both cases that we set the beam A (Ch2 and Ch3) polarizer at angles 0° and 45° degree. Otherwise, there should be underlying mechanism that affect the result and create the two distinguished results. Explanation based on QM taking into account entanglement would be that in the first measurement that the polarizer

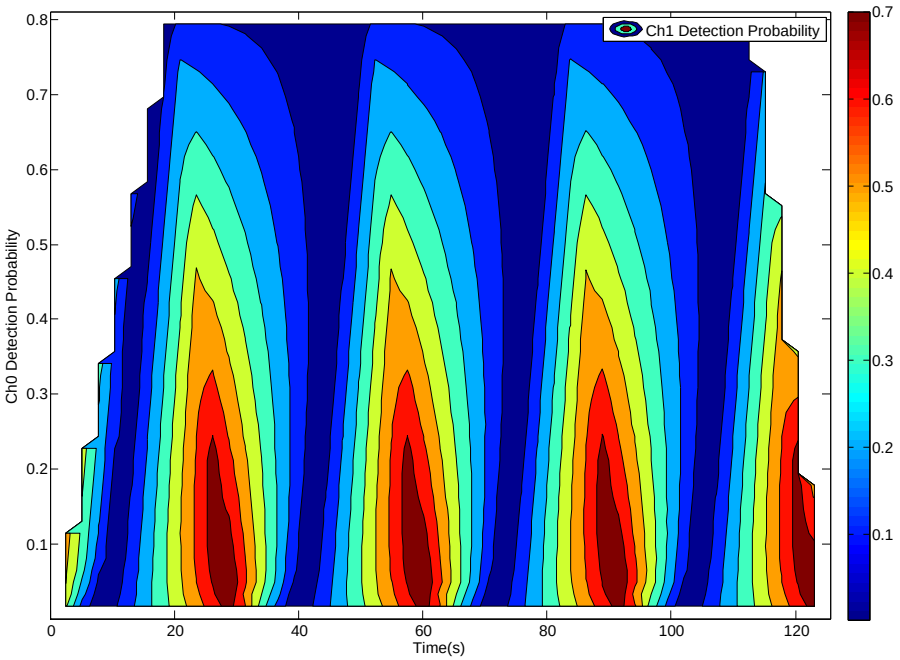

Figure 4: SPDC photon pair detection probability: Polarizer LP1' transmission axis set to horizontal by setting $\theta_1' = 0$ and varied the angle θ_1 of the second polarizer from 0 to 4π.

in channel 2 and 3 set to horizontal it will project the incoming photons states in to a well define state which simultaneously collapse the channel Z photons states into a well define state with a precise detection probability because the apparatus associates a distinct polarization state with each possible path: $|H\rangle$ for one path and $|V\rangle$ for the other. We can erase the distinguishability of states in both beam path by projecting the generated two orthogonal states with a half waveplate set to $\pi/4$ relative to the polarizer transmission axis. The projection amplitudes between $|H\rangle$, $|V\rangle$ and the polarizer state $|T_{45^\circ}\rangle$ are the equal. The state of each photon after such is

$$|T_\theta\rangle \left(\langle T_\theta \,|\, H\rangle + \langle T_\theta \,|\, V\rangle\right) \tag{5.3}$$

However, in the second measurement when the LP1' polarizer is set at the 45° degree. This 45° polarized light is then split at a polarizing beam-splitter which has a single-photon detector in each output. The PBS in this case acts as a 50:50 beamsplitter on the 45° polarized photons. The detected state will be random due to equal probability for collapse of the incoming photons into states defined by the PBS. Therefore, the random probability of the state collapse in beam A modifies the state collapse and counts distribution of photons in beam Z and in turn the detection probability for Ch0 and Ch1 changes. Hence, two photons cannot be further be distinguished, and the light can essentially be described by an entangled state. Thus the polarization of both photons is not independent which provides evidence of a non-real and nonlocal underlying mechanism.

In conclusion, the investigation of biphoton polarization correlation has been performed by fixing one beam polarizer setting at different angles and continuously rotating the polarizer placed in the second beam path in order to observe the distribution of single counts and biphoton polarization correlation. The biphoton signals were degenerated in frequency and entangled in polarization which were generated in type-II SPDC process in 10 mm long ppKTP-crystals pumped at 397nm. There is shown evidence for biphoton polarization with a substantial visibility contrast between orthogonal $|H\rangle$ and $|V\rangle$ detected states counts distributions. Further measurement of density matrix and reconstruction the tomographic data in next stage will reveal more information about the generated state and paves the way toward fidelity measure of states in optical setup after coupling to plasmonic nano-structures.

6. Acknowledgments

To whom inspire and live outside the box.

I am grateful to Niek F. Van Huslt for being the light and accepting the experiments proposal in such a short time with his continuous support during the research. He has been a source of inspiration for me to go beyond the limits and think outside the box. Moreover, I would like to thank all members of Molecular Nanophotonics group at ICFO and A. Esteban-Martin, M. Cristiani, F. Steinlechner, V. Ramaiah-Badarla for their support and insightful discussions which paved the way for constructing experimental setups from scratch.

This work is supported by the ERC – European Research Council, Advanced Grant ERC247330 - NanoAntennas and MICINN– Consolider Ingenio CSD2007-046 - NanoLight.

7. References

[1] D W Pohl, W Denk, and M Lanz. Optical stethoscopy: Image recording with resolution /20. *Applied Physics Letters*, 44(7):651, 1984.

[2] Michael J Rust, Mark Bates, and Xiaowei Zhuang. Sub-diffraction-limit imaging by stochastic optical reconstruction microscopy (STORM). *Nature Methods*, 3(10):793–796, August 2006.

[3] Eric Betzig, George H Patterson, Rachid Sougrat, O Wolf Lindwasser, Scott Olenych, Juan S Bonifacino, Michael W Davidson, Jennifer Lippincott-Schwartz, and Harald F Hess. Imaging Intracellular Fluorescent Proteins at Nanometer Resolution. *Science*, 313(5793):1642–1645, January 2006.

[4] Richard P Feynman. Simulating physics with computers. *International Journal of Theoretical Physics*, 21(6-7):467–488, June 1982.

[5] C H Bennett and G Brassard. Quantum cryptography: Public key distribution and coin tossing. In *Proceedings of IEEE International . . .*, 1984.

[6] Charles H Bennett, Gilles Brassard, Claude Crépeau, Richard Jozsa, Asher Peres, and William K Wootters. Teleporting an unknown quantum state via dual classical and Einstein-Podolsky-Rosen channels. *Physical Review Letters*, 70(13):1895–1899, March 1993.

[7] Dik Bouwmeester, Jian-Wei Pan, Klaus Mattle, Manfred Eibl, Harald Weinfurter, and Anton Zeilinger. Experimental quantum teleportation. *Nature*, 390(6660):575–579, December 1997.

[8] M Riebe, H Häffner, C F Roos, W Hänsel, J Benhelm, G P T Lancaster, T W Körber, C Becher, F Schmidt-Kaler, D F V James, and R Blatt. Deterministic quantum teleportation with atoms. *Nature*, 429(6993):734–737, June 2004.

[9] E Schrödinger. Die gegenwärtige Situation in der Quantenmechanik. *Die Naturwissenschaften*, 23(49):823–828, December 1935.

[10] A Einstein. Can Quantum-Mechanical Description of Physical Reality Be Considered Complete? *Physical Review*, 47(10):777–780, January 1935.

[11] J S Bell. On the einstein-podolsky-rosen paradox. *Physics*, 1964.

[12] D Bohm and Y Aharonov. Discussion of Experimental Proof for the Paradox of Einstein, Rosen, and Podolsky. *Physical Review*, 108(4):1070–1076, November 1957.

[13] Stuart J Freedman and John F Clauser. Experimental Test of Local Hidden-Variable Theories. *Phys.Rev.Lett.*, 28:938–941, 1972.

[14] Alain Aspect, Jean Dalibard, and Gérard Roger. Experimental Test of Bell's Inequalities Using Time- Varying Analyzers. *Physical Review Letters*, 49(25):1804–1807, December 1982.

[15] J F Clauser, M A Horne, A Shimony, and R A Holt. Propesed Experiment to Test Local Hidden-Variable Theories . *Physical Review Letters*, 1969.

[16] John F Clauser and Michael A Horne. Experimental Consequences of Objective Local Theories. *Phys.Rev.*, D10:526, 1974.

[17] Karl Blum. *Density Matrix Theory and Applications*. Springerverlag Berlin Heidelberg, January 2012.

[18] Bao-Sen Shi and Akihisa Tomita. Generation of a pulsed polarization entangled photon pair using a Sagnac interferometer. *Physical Review A*, 69(1):013803, January 2004.

[19] Taehyun Kim, Marco Fiorentino, and Franco N C Wong. Phase-stable source of polarization-entangled photons using a polarization Sagnac interferometer. *Physical Review A*, 73(1):012316, January 2006.

[20] Alessandro Fedrizzi, Thomas Herbst, Andreas Poppe, Thomas Jennewein, and Anton Zeilinger. A wavelength-tunable fiber-coupled source of narrowband entangled photons. *Optics Express*, 15(23):15377–15386, November 2007.